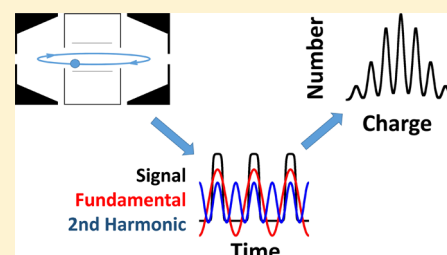


Charge Detection Mass Spectrometry with Almost Perfect Charge Accuracy

David Z. Keifer, Deven L. Shinholt, and Martin F. Jarrold*

Chemistry Department, Indiana University, 800 East Kirkwood Avenue, Bloomington, Indiana 47401, United States

ABSTRACT: Charge detection mass spectrometry (CDMS) is a single-particle technique where the masses of individual ions are determined from simultaneous measurement of each ion's mass-to-charge ratio (m/z) and charge. CDMS has many desirable features: it has no upper mass limit, no mass discrimination, and it can analyze complex mixtures. However, the charge is measured directly, and the poor accuracy of the charge measurement has severely limited the mass resolution achievable with CDMS. Since the charge is quantized, it needs to be measured with sufficient accuracy to assign each ion to its correct charge state. This goal has now been largely achieved. By reducing the pressure to extend the trapping time and by implementing a novel analysis method that improves the signal-to-noise ratio and compensates for imperfections in the charge measurement, the uncertainty has been reduced to less than $0.20 e$ rmsd (root-mean-square deviation). With this unprecedented precision peaks due to different charge states are resolved in the charge spectrum. Further improvement can be achieved by quantizing the charge (rounding the measured charge to the nearest integer) and culling ions with measured charges midway between the integral values. After ions with charges more than one standard deviation from the mean are culled, the fraction of ions assigned to the wrong charge state is estimated to be 6.4×10^{-5} (i.e., less than 1 in 15 000). Since almost all remaining ions are assigned to their correct charge state, the uncertainty in the mass is now almost entirely limited by the uncertainty in the m/z measurement.



The use of electrospray mass spectrometry to analyze macromolecules and supramolecular assemblies is hindered by heterogeneity. Heterogeneity, either intrinsic or from adduct formation, causes the loss of charge state resolution in the m/z (mass-to-charge ratio) spectrum, which in turn makes it impossible to deduce the mass. Several solutions based on measuring the m/z and charge of individual ions have been proposed. In the early 1990s, Smith and collaborators described a method where the m/z is measured for a single macroion, the charge is shifted, and then the m/z remeasured.^{1–4} The charge is deduced from the shifts in the m/z values, and then the mass is determined from the m/z values and the charges. Smith and collaborators used Fourier transform ion cyclotron resonance (FTICR) to measure the m/z values. Several groups have used a related method where the m/z values are determined using light scattering to interrogate the trajectory of a macroion in a quadrupole ion trap.^{5–10} However, these charge shifting approaches are better suited to monitoring the behavior of a single ion over a long period of time than to measuring the masses for the large number of ions needed to construct a mass spectrum.

Cryogenic detectors (superconducting tunnel junctions^{11–14} and microcalorimeters^{15–17}) generate a signal related to the energy deposited when an ion strikes the detector. They have been used as high-mass detectors mainly in MALDI-TOF (matrix-assisted laser desorption/ionization time-of-flight) spectrometers. Since the kinetic energy of an ion accelerated through a potential is proportional to its charge, cryogenic detectors can be used to measure the charge. However, the energy resolution is not currently sufficient to resolve the high

charge states found in electrospray, and MALDI, where the ions are less highly charged, is not the ionization method of choice for studies of supramolecular assemblies under native conditions.

In charge detection mass spectrometry (CDMS), the masses of individual ions are determined from direct measurement of each ion's charge and m/z . At the heart of this approach is a conducting cylinder connected to a charge-sensitive preamplifier. When an ion enters the cylinder it induces a charge which is detected by the preamplifier. If the cylinder is long enough, the induced charge equals the charge on the ion, and the transit time provides a measure of its velocity. If the energy per charge is known, the m/z can be determined from the velocity. The charge and m/z can then be combined to give the mass. This basic scheme was first used in 1960 to determine the masses of micrometer-sized particles for hypervelocity impact studies.^{18–20}

A key development occurred in the mid-1990s, when Fuerstenau and Benner used CDMS to perform mass measurements on electrosprayed ions with masses in the megadalton range.^{21–23} While ground-breaking, the mass resolution achieved in these early studies was low due to the poor accuracy of the charge measurement. The main factor limiting the accuracy is electrical noise. Fuerstenau and Benner reported a root mean square (rms) noise of 50 elementary charges (e). A more accurate value for the charge can be

Received: June 19, 2015

Accepted: September 18, 2015

Published: September 29, 2015

obtained by signal averaging, and Benner subsequently used a linear ion trap to repetitively measure the charge.²⁴ In the best case, an ion was trapped for 10 ms (450 cycles); the rms noise was reduced by averaging to 2.3 *e*. Surprisingly, Benner did not follow up on this breakthrough. Recently, Antoine, Dugourd, and collaborators used a trap similar to Benner's for a variety of polymer and nanoparticle applications that did not require precise charge measurements.^{25–27}

In recent papers,^{28–33} we have described some key improvements to CDMS. By using fast Fourier transforms to analyze the time domain signals,²⁸ by cryogenic cooling of the junction gate field-effect transistor (JFET) used to detect the signal,²⁹ and by extending the trapping time to 400 ms,³³ the limit of detection has been lowered to below 7 *e* and the uncertainty (rmsd) in the charge measurement has been reduced to 0.65 *e*. However, even with these improvements, CDMS is still hindered by low mass resolution.

Since the charge is quantized, the goal is to measure it with sufficient accuracy that the true charge state of each ion can be determined with complete confidence. This would remove any remaining uncertainty in the charge measurement, in which case the mass resolution would only depend on the *m/z* measurement. Realizing this goal requires that the uncertainty in the charge is reduced to the point where there are baseline-resolved peaks in the charge spectrum due to different charge states.

In this manuscript we report that the goal of perfect charge accuracy has almost been achieved. By lowering the background pressure by 2 orders of magnitude we have been able to extend the trapping time to 3 s. In addition, we have developed a novel scheme for analyzing the experimental time domain data where harmonics are used to improve the signal-to-noise ratio and correct for variations in the magnitude of the charge due to differences in the ion's trajectory and kinetic energy. With these upgrades, the root-mean-square deviation (rmsd) has been reduced to below 0.2 *e*. Further improvement in the accuracy can be achieved by quantizing the charge (rounding the measured charge to the nearest integer) and culling ions with measured charges midway between the integral values (the ions that are most likely to be assigned to the wrong charge state). This procedure can only be performed if there are well-resolved peaks in the charge spectrum, which we have achieved in this work for the first time. After quantizing and culling ions with charges more than one standard deviation from the mean, the fraction of ions assigned to the wrong charge state is estimated to be 6.4×10^{-5} (i.e., less than 1 in 15 000). In other words, almost all the ions are assigned to the correct charge state.

■ EXPERIMENTAL METHODS

Our charge detection mass spectrometer has been described in detail elsewhere.^{28–30,33} The main modification for this work is the addition of another stage of differential pumping which lowered the operating pressure in the trap region by 2 orders of magnitude. The lower pressure allowed a substantial increase in the trapping time. A brief description of the instrument is given below.

Ions are generated by nanoelectrospray and enter the vacuum chamber by passing through a heated capillary. They are transmitted through three differentially pumped regions containing an ion funnel, a hexapole, and a quadrupole operated in rf-only mode. A 100 V dc offset on the hexapole rods sets the nominal ion energy. At the end of the quadrupole, an einzel lens focuses the ions into the entrance of a dual

hemispherical deflection analyzer (HDA). The HDA is a kinetic energy filter that is configured to only transmit ions within a narrow band centered on 100 eV/charge (eV/*z*). The transmitted ions are then focused into a modified cone trap which bookends the charge detection cylinder. We have recently added a dividing wall between the HDA and the ion trap and added pumps so that the ion trap can be differentially pumped. To avoid electrical and mechanical noise, the ion trap region is pumped with an Edwards Diffstak, which was modified to operate in the ultrahigh vacuum (UHV) regime. With the differential pumping, the operating pressure in the trap has been improved by 2 orders of magnitude to $<3 \times 10^{-9}$ mbar, reducing the frequency of collisions with the background gas by the same factor.

When the end-caps of the ion trap are grounded, ions fly through the trap and strike a pair of microchannel plates used to monitor the signal. To close the trap, the potential on the back end-cap is raised to 135 V, and 0.5 ms later, the potential on the front end-cap is raised to the same value. A trapped ion oscillates back and forth, passing through the central charge detection cylinder. As the ion passes through the cylinder it induces a charge which is detected by a cryogenically cooled JFET (2SK152) at the input of a charge-sensitive preamplifier (Amptek A250). The output from the preamplifier is transferred outside the vacuum chamber where it is digitized and stored for off-line analysis. At the end of the trapping period the end-caps are grounded to release the ion and initiate a new trapping cycle.

Measurements were performed with rabbit muscle pyruvate kinase (Lee Biosolutions) at 2.5 mg/mL in 100 mM ammonium acetate ($\geq 99.99\%$, Sigma-Aldrich). The sample was purified by size exclusion chromatography before use. Pyruvate kinase primarily exists as a tetramer in solution,³⁴ although further aggregation has been observed.³⁰

The maximum trapping time is set by the pulse sequence provided to the trap. In our previous work, about 70% of the pyruvate kinase ions were trapped for 391 ms (the maximum trapping time used in those experiments). With the lower pressure, about 87% of the pyruvate kinase ions are trapped for at least 391 ms, and about 82% are trapped for 2991 ms (the maximum trapping time used here). At the lower pressure, most of the ions trapped for a few hundred milliseconds remain trapped for much longer. Some of the ions are probably trapped for much longer than 2991 ms, though this was not investigated. Those trapped for only a short time may enter the trap severely off-axis or off-angle so that a few collisions with background gas molecules nudge their trajectories into instability.

■ ANALYSIS OF EXPERIMENTAL DATA

The stored time domain signals are analyzed using fast Fourier transforms (FFTs). The frequency of the ion's oscillation in the trap is related to its *m/z*, and the amplitude of the signal is related to the charge. First, an FFT is performed for the whole trapping event. The result is used to determine whether the trap is empty (i.e., no peak in the frequency domain spectrum rises above a predetermined threshold) or whether it contains single or multiple ions. If a single ion is present, the peaks in the frequency spectrum due to the fundamental and higher-order harmonics are evenly spaced. With multiple ions they are irregularly spaced. The empty and multiple ion trapping events are discarded. For the remaining single-ion trapping events, the next step is to determine how long each ion is trapped. Short,

Gaussian-apodized FFTs are stepped across the time domain signals, and the peaks in the FFT disappear if the ion leaves the trap before the end of the trapping event. The frequency and magnitude are extracted from each short FFT, and the results from all FFTs are averaged up until the point where the ion leaves the trap (if it is not trapped for the full period).

The relationship between the ion's fundamental frequency and its m/z is

$$\frac{m}{z} = \frac{C}{f^2} \quad (1)$$

where C is a constant determined from Simion simulations. C depends on the geometry of the ion trap, the voltages on it, and the ion energy. The charge is determined from the magnitude of the peaks in the frequency spectrum. The charge is calibrated by loading simulated signals into a function generator and applying them through a known capacitance into the input of the JFET. From the amplitude of the signal from the function generator and the capacitance, the charge deposited on the input of the JFET can be calculated. This charge is then compared to the magnitude of the peaks in the FFT of the amplified signal to obtain the calibration factor. This calibration must be performed with relatively large charges, typically between 2000 and 10 000 e . As we describe below, a much more accurate calibration is possible here because we have achieved resolution in the charge spectrum for ions with 30–80 charges. The more accurate calibration reduced the charge calibration factor by 1.25%, and this value has been used for all the results reported here.

Figure 1a shows 400 ms of the time domain signal for a 16-mer of pyruvate kinase. Analysis of this signal shows that the

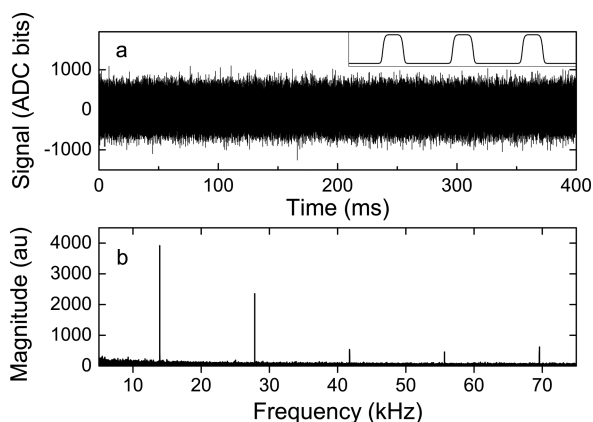


Figure 1. (a) Time domain signal for a 16-mer of pyruvate kinase trapped for 400 ms. The inset shows an expanded view of a simulated signal of an ion oscillating along the trap axis (the axes of the simulated signal are not to scale). (b) Fast Fourier transform of the signal shown in part a. The fundamental frequency is at around 13.9 kHz. Higher-frequency peaks are harmonics resulting from the nonsinusoidal nature of the signal (see inset).

ion has around 72 charges. While this is larger than the noise, it is not much larger, and the signal-to-noise ratio is relatively low. An expanded view of a the time domain signal shows oscillations due to the induced charge but does not reveal much about the shape of the underlying signal. The inset in Figure 1a shows a simulated signal for an ion oscillating along the center axis of the trap (the axes are not to scale). The signal is trapezoidal, with rise and fall times of around 5% of the signal

period and a duty factor of around 30%. The rise and fall times are dictated by the time it takes for ions to enter and exit the detection tube. The duty factor is determined by the trap geometry. With the trap employed here, an ion spends around 30% of its time traveling through the detector tube and around 70% traveling outside; during this time it slows down, reverses direction, and accelerates back toward the detection tube. The signal repeats with constant amplitude (except for the effect of noise) until the trapping period ends or the ion is lost from the trap, at which point the signal disappears. This is unlike other types of Fourier transform mass spectrometry, such as FTICR, where the signal decays over time as a result of dephasing and collisional cooling. The difference results because CDMS is a single-ion technique.

Figure 1b shows an FFT of 400 ms of the experimental time domain data in Figure 1a. The peak at 13.9 kHz is the fundamental. All the other peaks are higher-order harmonics which are prevalent because the signal is far from sinusoidal, as is evident from the inset in Figure 1a.

Since a substantial fraction of our signal appears as higher-order harmonics, we sought to use them to improve the charge measurement. We first investigated this possibility with simulations. Noise files were generated by collecting data with everything running except for the electrospray source. A simulated signal for an ion with an m/z of 12 500 Th and a charge of 60 e oscillating along the trap axis with an energy of 100 eV/ z was then added to 10 000 noise files with a simulated trapping time of 95 ms. The files were analyzed using FFTs to determine the magnitudes of the fundamental and the harmonics. The magnitude of the second harmonic was, on average, 60.4% of the magnitude of the fundamental. This is typical of what we see for real ions as well, as evident from Figure 1b. Because the second harmonic is so large, adding its magnitude to the fundamental improves the signal-to-noise ratio, which translates into a more precise charge measurement. The rmsd for these 95 ms simulations was 1.37 e when just the fundamental was used and 1.06 e when the first two harmonics were summed, a 23% reduction in the uncertainty. The relatively low precision found here results from the short trapping time that was used in the simulations. We have seen that the uncertainty in the charge decreases as one over the square root of trapping time.³³ Adding the first two harmonics should improve the charge measurement for longer trapping times by at least the same proportion.

Since summing the first two harmonics yields a more precise charge measurement than just the fundamental, we investigated whether adding more harmonics was even better. We generated test signals with m/z ranging from 6 to 100 kTh and charges ranging from 100 to 500 e and added them to 10 000 noise files. We analyzed the data by summing many combinations of harmonics, but no combination led to a reliably more precise charge measurement across the range of input m/z and charge than just using the first two harmonics. This is because the higher harmonics are less intense, so the noise which also gets added with higher harmonic signals prevents the signal-to-noise ratio from improving significantly.

As noted above, the main contributor to the uncertainty in the charge measurement is electrical noise. However, at very long trapping times where the contribution of the noise has been substantially diminished by averaging, other sources of uncertainty may emerge. The simulations described above were performed for ions that oscillated along the trap axis with a kinetic energy of precisely 100 eV/ z . For ions that have

different kinetic energies, the duty cycle (i.e., the ratio of the time spent in the charge detection cylinder over the total time to complete one cycle) is slightly different. Slightly different duty cycles lead to slightly different magnitudes for the peaks from the FFTs and, hence, slightly different charges. The black points in Figure 2 shows a plot of the charge determined from

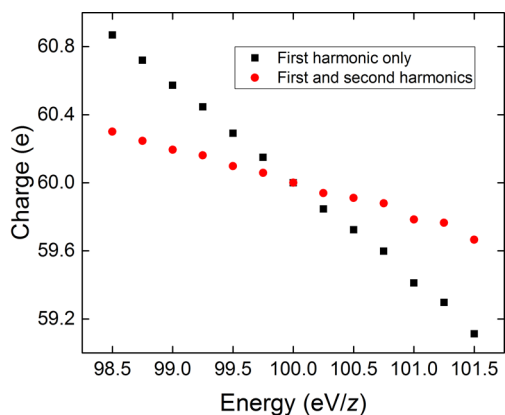


Figure 2. Plot of the charge determined as a function of the kinetic energy per charge. The results are from simulated signals for ions oscillating along the trap axis. The ions had 60 charges and an m/z of 12 500 Th. The charge was determined from the magnitude of the first harmonic only (black squares) and from the sum of the magnitudes of the first and second harmonics (red circles).

the FFT fundamental as a function of kinetic energy per charge. These results are from simulations for ions with a charge of 60 e and an m/z of 12 500 Th oscillating on the trap axis with kinetic energies from 98.5 to 101.5 eV/z. This range of kinetic energies is around three times broader than the distribution present in the experiments (where the fwhm is around 1 eV/z). The charges determined from the FFT fundamentals decrease significantly as the kinetic energy is raised. The correct charge is recovered at a kinetic energy of 100 eV/z because this is where the calibration was performed. The red points in the figure show the charge determined from both the fundamental and second harmonic. With the second harmonic, the dependence of the charge on the kinetic energy is reduced by close to a factor of 3.

In addition to the ion's kinetic energy, the trajectory of the ion in the trap also affects the duty cycle. Instead of entering along the trap axis, as we assumed above, most ions enter the trap slightly off-axis and at a small angle to the trap axis. The ion then follows a complex trajectory reminiscent of Lissajous figures. The duty cycle for these trajectories is slightly larger than for on-axis oscillation because the ion spends less time reflecting outside the detector tube. The black points in Figure 3 show the charge determined from the fundamental for ions that are created at the center of the trap as a function of the radial offset. The ions have a charge of 60 e , an m/z of 12 500 Th, and a kinetic energy of 100 eV/z. As the offset increases the charge deviates further from the input value of 60 e because the duty cycle increases relative to the value for oscillation along the trap axis. The red points in Figure 3 show the charge determined from the fundamental and the second harmonic. The variation in the charge with angle is reduced relative to the value determined from the fundamental alone. In this case, the decrease is not as large as it was with the energy, but it is still substantial. We also investigated trajectories where ions were generated at the center of the trap with a small angle to the trap

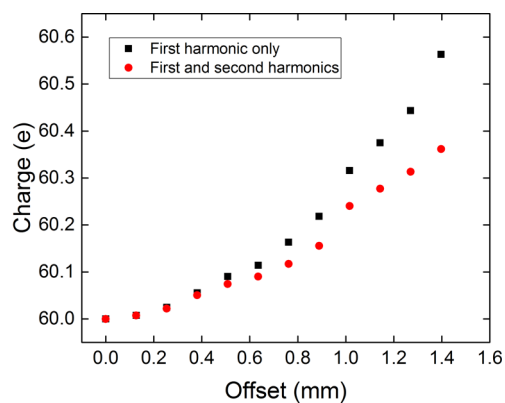


Figure 3. Plot of the charge determined as a function of the radial offset from simulated signals for ions with 60 charges, an m/z of 12 500 Th, and a kinetic energy per charge of 100 eV/z. The charge was determined from the magnitude of the first harmonic only (black squares) and from the sum of the magnitudes of the first and second harmonics (red circles).

axis. The results (not shown) are similar to those in Figure 3 for the radial offset.

The results presented above show that significant errors result in the charge determined from the fundamental when the duty cycle deviates from the value used to calibrate the signal. However, these errors can be mitigated by adding the magnitudes of the fundamental and the second harmonic. Summing the magnitudes of the first and second harmonic also improves the signal-to-noise ratio which in turn improves the precision of the charge measurement. Thus, according to the simulations, adding the first and second harmonic increases both the accuracy and the precision of the charge measurements.

To test the performance of the new data analysis scheme we reanalyzed our pyruvate kinase data measured with a trapping time of 391 ms and found that adding the magnitude of the first and second harmonics reduced the charge uncertainty from 0.65 to 0.49 e . This improvement is in line with the improvement found in the simulations described above. The improvement results mainly from the increased signal-to-noise ratio. The duty cycle effects become more significant for more highly charged ions (see below).

EXPERIMENTAL RESULTS

With the lower pressure in the trap region, 82% of pyruvate kinase ions were trapped for the full 2991 ms. Ions trapped for less than the full trapping period were discarded. The sum of the magnitudes of the first and second harmonics was used to determine the charge. The resulting charges were binned to generate a histogram. A portion of the histogram generated using 0.2 e bins is shown in Figure 4. There are oscillations in the histogram which result from resolution of the charge states. In other words, the charge is measured with sufficient accuracy and precision that ions with n charges are well-resolved in the charge spectrum from those with $n - 1$ and $n + 1$. The groups of peaks in Figure 4 are due to pyruvate kinase in different states of oligomerization. The group centered around 33–34 charges is due to the pyruvate kinase tetramer, $(PK_4)_2$. The group centered around 47 charges is due to the octamer, $(PK_4)_2$, and the group centered around 58–59 charges is due to the dodecamer, $(PK_4)_3$.

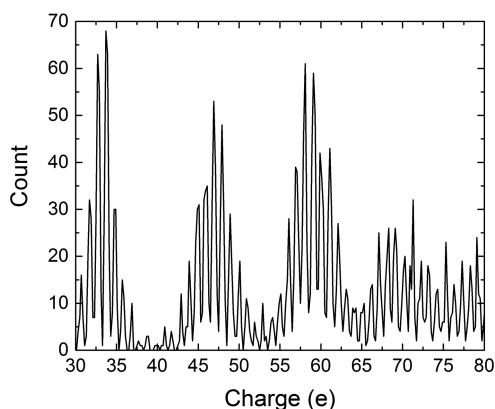


Figure 4. Partial charge histogram for pyruvate kinase ions trapped for 2991 ms. The charges were determined from the sum of the first two harmonics. The bin width is $0.2 e$, and the histogram contains 3125 ions.

To obtain better information on resolution of the charge measurements we generated a composite charge histogram by binning the measured charges into $0.05 e$ bins and then summing the bins for charges from 30 to $51 e$ (which covers the peaks due to the tetramer and octamer in Figure 4). Using this procedure, the composite bin centered on $0.025 e$ is the sum of bins centered on 30.025 , 31.025 , 32.025 , and so on up to $51.025 e$. The composite histogram obtained in this way is shown by the blue points in Figure 5. We used only the

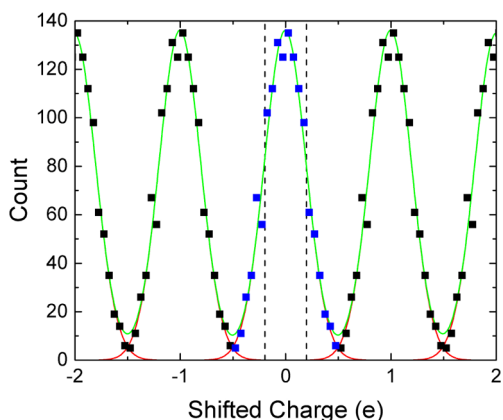


Figure 5. Composite charge histogram obtained by binning into $0.05 e$ bins and then summing charge states 30–51 (blue points). The black points show the composite histogram offset by -2 , -1 , $+1$, and $+2$ charges. The green line is a least-squares fit of a series of Gaussians (shown by the red lines) to the composite spectrum. The vertical dashed lines are one standard deviation from the center of the central peak.

tetramer and octamer peaks to generate the composite histogram so that the results can be directly compared to our previous work.³³ In our previous work, information on the charge rmsd was derived using the m/z charge states, and we only had resolved charge states in the m/z spectrum for the tetramer and octamer. The black points in Figure 5 show the composite spectrum offset by -2 , -1 , $+1$, and $+2$ charges. The green line is a least-squares fit of a series of Gaussians (shown by the red lines) to the composite spectrum. The standard deviation that yields the best fit is $0.196 e$. The agreement between the Gaussian fit and the composite spectrum is

excellent. An uncertainty of $0.196 e$ is more than a factor of 3 improvement over the previous best ($0.65 e$); however, as described below, a much larger improvement can be now realized because the charge states are resolved for the first time.

The charge determined in CDMS is not an integer, but it can be quantized by assigning it the value of the nearest integer. In all previous CDMS experiments (where the uncertainty was greater than or equal to $0.65 e$) the charges were not quantized and the measured values were used. Quantizing the charge in these cases would have degraded the overall accuracy of the charge measurement. This can be demonstrated by taking a Gaussian charge distribution, assigning the charge to the nearest integer value, and then determining the rmsd. The solid red line in Figure 6a shows the rmsd of the quantized charges

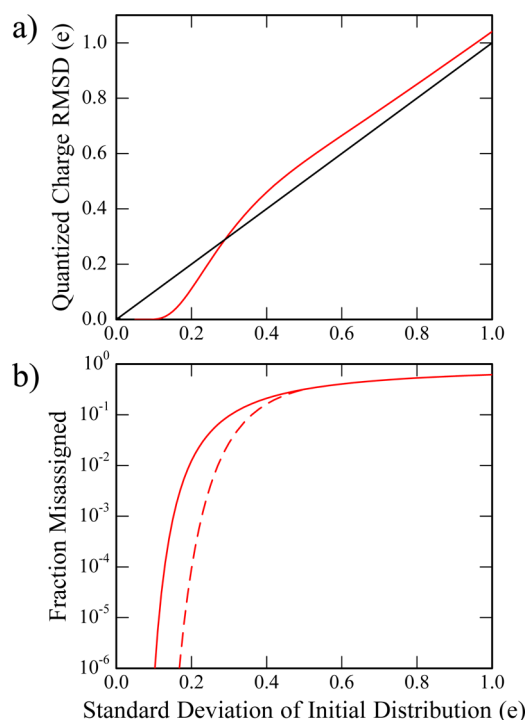


Figure 6. (a) The rmsd after assigning the charge to the nearest integer value plotted against the standard deviation of the initial Gaussian distribution (red line). The black line is a guide showing a linear relationship between the quantized charge rmsd and the standard deviation of the initial distribution. (b) The fraction of ions assigned to the wrong charge state as a function of the standard deviation of the initial distribution (solid red line). The dashed red line shows the fraction misassigned after ions more than one standard deviation from the mean are discarded.

plotted against the standard deviation of the initial Gaussian distribution. The black line is a guide showing a linear relationship. For standard deviations greater than around $0.3 e$, quantizing the charges increases the rmsd (i.e., makes the charge less accurate on average). For standard deviations less than $0.3 e$, however, the rmsd drops sharply and vanishes. With quantized charges, it is more appropriate to think in terms of the fraction of ions that have their charge assigned to the wrong integer value than the rmsd. This fraction is plotted as the solid red line in Figure 6b. If the standard deviation of the initial Gaussian distribution is $0.196 e$ (as in the experiments) the fraction of ions assigned to the wrong charge state is around 0.010. The ions with the highest probability of being

misassigned have charges that lie halfway between two integer values. For example, if an ion has a measured charge of $37.5 e$ there is almost a 50/50 chance that it will be misassigned. The overall accuracy of the charge measurements can be dramatically improved by discarding ions with measured charges that are midway between two integer values. The dashed red line in Figure 6b shows the result of culling charges that are more than one standard deviation from the integer values (see vertical dashed lines in Figure 5). With this procedure, around a third of the ions are culled, but the fraction that is misassigned drops precipitously. For an initial standard deviation of $0.196 e$, the fraction misassigned drops from around 1.0×10^{-2} to around 6.4×10^{-5} , an improvement of more than 2 orders of magnitude. If we expand the window to include ions with measured charges within two standard deviations of the mean (95% of the ions fall in this window) the fraction of incorrectly assigned charges is 2.0×10^{-3} . Just discarding 5% of the ions reduces the fraction misassigned by a factor of 5.

It is evident that a dramatic improvements in the accuracy of the charge measurement can be realized by quantizing the charge and culling ions with measured charges that are close to midway between two integer values. However, this procedure requires well-resolved charge states in the charge spectrum, and this is the first time that the charges were measured with sufficient precision to implement it. Most CDMS spectra contain a few thousand ions, so with 6.4×10^{-5} of the ions misassigned (i.e., less than 1 in 15 000), many of the spectra measured under these conditions will have charges that are perfectly accurate.

Figure 7 shows the mass histogram obtained by multiplying the measured m/z for each ion by its assigned integral charge.

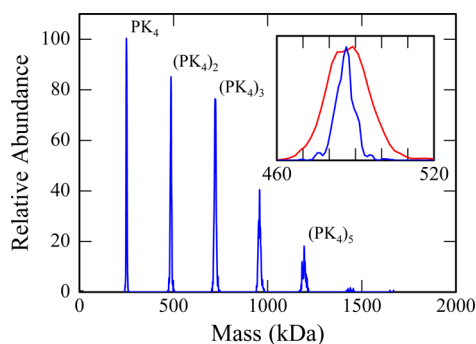


Figure 7. Pyruvate kinase mass histogram obtained by assigning an integer value to the charge of each ion with a measured charge within one standard deviation of the mean, multiplying the measured m/z by the integer charge to obtain the mass, and then binning the masses into 1 kDa bins. The spectrum contains 2098 ions. The peak at ~ 240 kDa is due to the tetramer, and the peak at 480 kDa is due to the octamer. The inset shows an expanded view of the octamer peak (blue line). The red line in the inset is the octamer peak from our previous work where the uncertainty in the charge was $0.65 e$ (binned using 2 kDa bins).

The spectrum contains 2098 ions, and so there is a high probability (more than 80%) that all the ions in the spectrum have their charge states assigned correctly. The peaks at around 240 and 480 kDa are due to the tetramer and octamer, respectively. Peaks can be seen up to the expected mass for the 24-mer, $(PK_4)_6$. The inset in the figure shows an expanded view of the peak for the octamer. The red line shows the octamer

peak measured with a charge uncertainty of $0.65 e$ (from our previous work³³). The blue line shows the peak measured with almost perfect charge accuracy (this work). The blue peak is 2.4 times narrower than the red; however, it is still fairly broad. The main factor determining the width of the blue peak is not the uncertainty in the charge (because this has been almost entirely removed), but the uncertainty in the m/z measurement.

DISCUSSION

In other mass spectrometry techniques that use a Fourier transform to convert from the time to the frequency domain, such as FTICR and the Orbitrap, a single FT can provide information on many different chemical species. In these techniques, harmonics are usually a nuisance because they can confuse data interpretation and reduce the signal-to-noise ratio. Efforts to identify which peaks are real and which are from harmonics have been made to avoid the issue.^{35,36} Harmonics have occasionally been useful. In FTICR, for example, it is possible to determine the energies of the ions from the relative magnitudes of the harmonics in the FT.³⁷ Also, under certain conditions the peak widths of higher harmonics in the FT equal the width of the fundamental peak. In these cases, using the higher harmonics to analyze the spectrum can lead to improved resolution.^{38,39} To the best of our knowledge, this is the first time that the magnitudes of the harmonics have been summed to improve the quality of the data analysis.

The substantial reduction in charge uncertainty achieved here is an important breakthrough in CDMS because it results, for the first time, in well-resolved peaks in the charge spectrum, allowing the true charge state to be assigned for almost all of the ions. While the improvement in the charge rmsd from the previous best (0.65 to $0.196 e$) is only a little over a factor of 3, reducing the rmsd to the point where the charges are resolved allows the charges to be quantized and ions with intermediate charges to be culled. Quantizing the charge reduces the effective rmsd from 0.196 to $0.11 e$, and culling ions more than one standard deviation from the mean reduces it further to $0.0080 e$. The net result is an 800-fold improvement in the accuracy of the charge measurement. For perfect charge accuracy, all the ions must be assigned to their correct charge state. While perfect accuracy may not be achievable in principle, it can be attained in practice by reducing the rate that ions are assigned to the wrong charge state to a value that is vanishingly small. The error rate obtained here is less than 1 in 15 000. While not quite vanishingly small, it is small enough to remove almost all of the uncertainty from the charge measurement, making the mass resolution almost entirely dependent on the uncertainty in the m/z measurement. The ion trap used here was not designed to optimize the m/z resolution, and the ion's oscillation frequency depends quite strongly on its kinetic energy per charge. The energy spread of the ions entering the trap is responsible for most of the uncertainty in the m/z . This is why the dramatically improved charge accuracy does not result in dramatically narrower peaks in the mass distributions (see the inset in Figure 7). Almost all of the frequency dependence on the kinetic energy can be removed by optimizing the design of the trap.⁴⁰

As outlined above, there are two main contributions to the uncertainty in the charge measurement: electrical noise and variations in the duty cycle due to the ion's trajectory and kinetic energy in the trap. Electrical noise dominates unless it is substantially reduced by averaging. The contribution to the uncertainty from the noise should be independent of charge

(i.e., the uncertainty should be the same whether the ion has a charge of 60 or 600 e). However, a charge dependence is introduced because heavier, more highly charged ions typically have higher m/z values. Ions with a higher m/z oscillate with a lower frequency, and the $1/f$ noise increases as the frequency decreases. Thus, the charge accuracy is slightly lower for heavier ions. For example, the average standard deviation of peaks from tetramer charge states (31–37 e) in Figure 4 is 0.18 e and from 16-mer charge states (67–72 e) it is 0.22 e . The other contribution to the uncertainty in the charge, the variation in the duty cycle, is expected to contribute an uncertainty that scales with the charge. So while this contribution is minor for an ion with 60 charges, it will become more important as the charge increases. Thus, it will be more difficult to obtain charge state resolution for much more highly charged ions than examined here because of their lower oscillation frequency and the stronger effects from the duty cycle.

CONCLUSIONS

We have substantially reduced the uncertainty of the charge measurement in CDMS by extending the trapping time to 3 s (up to 60 000 oscillations) and improving the data analysis. Summing the magnitudes of the fundamental and second-harmonic peaks in the FFT both improves the signal-to-noise ratio and mitigates the effect on the charge measurement of different ion trajectories and energies within the trap. After these improvements, the uncertainty in the charge was sufficiently small that almost baseline-resolved peaks were observed in the charge spectrum of pyruvate kinase. With well-resolved peaks, it is appropriate to assign an integer charge to each ion. The fraction of ions with misassigned charges can be dramatically reduced by culling ions with measured charges halfway between the integer values. In the present work, ions with charges more than one standard deviation from the mean were discarded, resulting in an error rate of less than 1 in 15 000. CDMS spectra typically contain a few thousand ions, so with this low error rate, many spectra will contain charges that are perfectly accurate. The uncertainty in the mass is then almost entirely determined by the uncertainty in the m/z measurement.

AUTHOR INFORMATION

Corresponding Author

*E-mail: mfj@indiana.edu.

Notes

The authors declare no competing financial interest.

ACKNOWLEDGMENTS

We gratefully acknowledge the support of the National Science Foundation through Award No. 0832651. We would also like to thank Mr. John Poehlmann and Mr. Andy Alexander in Electronic Instrument Services and Mr. Delbert Allgood in Mechanical Instrument Services for their technical assistance.

REFERENCES

- (1) Cheng, X.; Bakhtiar, R.; Van Orden, S.; Smith, R. D. *Anal. Chem.* **1994**, *66*, 2084–2087.
- (2) Bruce, J. E.; Cheng, X.; Bakhtiar, R.; Wu, Q.; Hofstadler, S. A.; Anderson, G. A.; Smith, R. D. *J. Am. Chem. Soc.* **1994**, *116*, 7839–7847.
- (3) Smith, R. D.; Cheng, X.; Bruce, J. E.; Hofstadler, S. A.; Anderson, G. A. *Nature* **1994**, *369*, 137–139.

- (4) Chen, R.; Cheng, X.; Mitchell, D. W.; Hofstadler, S. A.; Wu, Q.; Rockwood, A. L.; Sherman, M. G.; Smith, R. D. *Anal. Chem.* **1995**, *67*, 1159–1163.
- (5) Schlemmer, S.; Illema, J.; Wellert, S.; Gerlich, D. *J. Appl. Phys.* **2001**, *90*, S410–S418.
- (6) Peng, W.-P.; Cai, Y.; Chang, H.-C. *Mass Spectrom. Rev.* **2004**, *23*, 443–465.
- (7) Schlemmer, S.; Wellert, S.; Windisch, F.; Grimm, M.; Barth, S.; Gerlich, D. *Appl. Phys. A: Mater. Sci. Process.* **2004**, *78*, 629–636.
- (8) Peng, W.-P.; Yang, Y. C.; Kang, M.-W.; Lee, Y. T.; Chang, H.-C. *J. Am. Chem. Soc.* **2004**, *126*, 11766–11767.
- (9) Peng, W.-P.; Yang, Y.-C.; Kang, M.-W.; Tzeng, Y.-K.; Nie, Z.; Chang, H.-C.; Chang, W.; Chen, C.-H. *Angew. Chem., Int. Ed.* **2006**, *45*, 1423–1426.
- (10) Howder, C. R.; Bell, D. M.; Anderson, S. L. *Rev. Sci. Instrum.* **2014**, *85*, 014104.
- (11) Twerenbold, D.; Vuilleumier, J.-L.; Gerber, D.; Tadsen, A.; van den Brandt, B.; Gillet, P. M. *Appl. Phys. Lett.* **1996**, *68*, 3503–3505.
- (12) Frank, M.; Mears, C. A.; Labov, S. E.; Benner, W. H.; Horn, D.; Jaklevic, J. M.; Barfknecht, A. T. *Rapid Commun. Mass Spectrom.* **1996**, *10*, 1946–1950.
- (13) Banner, W. H.; Horn, D. M.; Jaklevic, J. M.; Frank, M.; Mears, C.; Labov, S.; Barfknecht, A. T. *J. Am. Soc. Mass Spectrom.* **1997**, *8*, 1094–1102.
- (14) Wenzel, R. J.; Matter, U.; Schultheis, L.; Zenobi, R. *Anal. Chem.* **2005**, *77*, 4329–4337.
- (15) Hilton, G. C.; Martinis, J. M.; Wollman, D. A.; Irwin, K. D.; Dulcie, L. L.; Gerber, D.; Gillet, P. M.; Twerenbold, D. *Nature* **1998**, *391*, 672–675.
- (16) Rabin, M. W.; Hilton, G. C.; Martinis, J. M. *IEEE Trans. Appl. Supercond.* **2001**, *11*, 242–247.
- (17) Rabin, M. W.; Hilton, G. C.; Martinis, J. M. *J. Am. Soc. Mass Spectrom.* **2001**, *12*, 826–831.
- (18) Shelton, H.; Hendricks, C. D.; Wuerker, R. F. *J. Appl. Phys.* **1960**, *31*, 1243–1246.
- (19) Keaton, P. W.; Idzorek, G. C.; Rowton, L. J.; Seagrave, J. D.; Stradling, G. L.; Bergeson, S. D.; Collopy, M. T.; Curling, H. L.; McColl, D. B.; Smith, J. D. *Int. J. Impact Eng.* **1990**, *10*, 295–308.
- (20) Stradling, G. L.; Idzorek, G. C.; Shafer, B. P.; Curling, H. L.; Collopy, M. T.; Hopkins Blossom, A. A.; Fuerstenau, S. *Int. J. Impact Eng.* **1993**, *14*, 719–727.
- (21) Fuerstenau, S. D.; Benner, W. H. *Rapid Commun. Mass Spectrom.* **1995**, *9*, 1528–1538.
- (22) Schultz, J. C.; Hack, C. A.; Benner, W. H. *J. Am. Soc. Mass Spectrom.* **1998**, *9*, 305–313.
- (23) Fuerstenau, S. D.; Benner, W. H.; Thomas, J. J.; Brugidou, C.; Bothner, B.; Siuzdak, G. *Angew. Chem., Int. Ed.* **2001**, *40*, 541–544.
- (24) Benner, W. H. *Anal. Chem.* **1997**, *69*, 4162–4168.
- (25) Doussineau, T.; Kerleroux, M.; Dagany, X.; Clavier, C.; Barbaire, M.; Maurelli, J.; Antoine, R.; Dugourd, P. *Rapid Commun. Mass Spectrom.* **2011**, *25*, 617–623.
- (26) Doussineau, T.; Bao, C. Y.; Antoine, R.; Dugourd, P.; Zhang, W.; D'Agosto, F.; Charleux, B. *ACS Macro Lett.* **2012**, *1*, 414–417.
- (27) Doussineau, T.; Désert, A.; Lambert, O.; Taveau, J.-C.; Lansalot, M.; Dugourd, P.; Bourgeat-Lami, E.; Ravaine, S.; Duguet, E.; Antoine, R. *J. Phys. Chem. C* **2015**, *119*, 10844–10849.
- (28) Contino, N. C.; Jarrold, M. F. *Int. J. Mass Spectrom.* **2013**, *345–347*, 153–159.
- (29) Contino, N. C.; Pierson, E. E.; Keifer, D. Z.; Jarrold, M. F. *J. Am. Soc. Mass Spectrom.* **2013**, *24*, 101–108.
- (30) Pierson, E. E.; Keifer, D. Z.; Contino, N. C.; Jarrold, M. F. *Int. J. Mass Spectrom.* **2013**, *337*, 50–56.
- (31) Keifer, D. Z.; Pierson, E. E.; Hogan, J. A.; Bedwell, G. J.; Prevelige, P. E.; Jarrold, M. F. *Rapid Commun. Mass Spectrom.* **2014**, *28*, 483–488.
- (32) Pierson, E. E.; Keifer, D. Z.; Selzer, L.; Lee, L. S.; Contino, N. C.; Wang, J. C. Y.; Zlotnick, A.; Jarrold, M. F. *J. Am. Chem. Soc.* **2014**, *136*, 3536–3541.

- (33) Pierson, E. E.; Contino, N. C.; Keifer, D. Z.; Jarrold, M. F. *J. Am. Soc. Mass Spectrom.* **2015**, *26*, 1213–1220.
- (34) Loo, J. A. *J. Mass Spectrom.* **1995**, *30*, 180–183.
- (35) Qi, Y.; Witt, M.; Jertz, R.; Baykut, G.; Barrow, M. P.; Nikolaev, E. N.; O'Connor, P. B. *Rapid Commun. Mass Spectrom.* **2012**, *26*, 2021–2026.
- (36) Hilger, R. T.; Wyss, P. J.; Santini, R. E.; McLuckey, S. A. *Anal. Chem.* **2013**, *85*, 8075–8079.
- (37) Grosshans, P. B.; Shields, P.; Marshall, A. G. *J. Am. Chem. Soc.* **1990**, *112*, 1275–1277.
- (38) Pan, Y.; Ridge, D. P.; Rockwood, A. L. *Int. J. Mass Spectrom. Ion Processes* **1988**, *84*, 293–304.
- (39) Nikolaev, E. N.; Rakov, V. S.; Futrell, J. H. *Int. J. Mass Spectrom. Ion Processes* **1996**, *157–158*, 215–232.
- (40) Hogan, J. A.; Shinholt, D. L.; Jarrold, M. F. Indiana University, Bloomington, IN. Unpublished work, 2015.